Particle Collection Efficiency for Nylon Mesh Screens

Lorenzo G. Cena[1], **Bon-Ki Ku**[2], and **Thomas M. Peters**[1]

[1]The University of Iowa, Department of Occupational and Environmental Health, University of Iowa Research Campus, 100 IREH, Iowa City, IA 52242, USA

[2]Centers for Disease Control and Prevention (CDC), National Institute for Occupational Safety and Health (NIOSH), 4676 Columbia Parkway, MS-R3, Cincinnati, OH 45226, USA

Abstract

Mesh screens composed of nylon fibers leave minimal residual ash and produce no significant spectral interference when ashed for spectrometric examination. These characteristics make nylon mesh screens attractive as a collection substrate for nanoparticles. A theoretical single-fiber efficiency expression developed for wire-mesh screens was evaluated for estimating the collection efficiency of submicrometer particles for nylon mesh screens. Pressure drop across the screens, the effect of particle morphology (spherical and highly fractal) on collection efficiency and single-fiber efficiency were evaluated experimentally for three pore sizes (60, 100 and 180 μm) at three flow rates (2.5, 4 and 6 Lpm). The pressure drop across the screens was found to increase linearly with superficial velocity. The collection efficiency of the screens was found to vary by less than 4% regardless of particle morphology. Single-fiber efficiency calculated from experimental data was in good agreement with that estimated from theory for particles between 40 and 150 nm but deviated from theory for particles outside this size range. New coefficients for the single-fiber efficiency model were identified that minimized the sum of square error (SSE) between the values estimated with the model and those determined experimentally. Compared to the original theory, the SSE calculated using the modified theory was at least one order of magnitude lower for all screens and flow rates with the exception of the 60-μm pore screens at 2.5 Lpm, where the decrease was threefold.

Keywords

nylon mesh screens; nanoparticle collection efficiency; particle morphology; single-fiber efficiency

Introduction

Wire-mesh screens have been widely used to sample submicrometer particles from aerosol streams and for determination of particle size distributions (Gentry and Choudhary 1975; Emi et al. 1982; Fu et al. 1990). The compact surface with uniform thickness, fiber diameter, pore size, and packing density of wire screens provides a consistent airflow and uniform

Address correspondence to: Thomas M. Peters, The University of Iowa, Department of Occupational and Environmental Health, University of Iowa Research Campus, 121 IREH, Iowa City, Iowa, 52242-5000, thomas-m-peters@uiowa.edu.

particle collection (Cheng 2001). Stainless steel wire screens are useful as diffusion cell material in screen-type diffusion batteries for measuring number, mass, or radioactivity concentrations at the inlet and outlet of each cell (Sinclair and Hoopes 1975; Yeh et al. 1982; Cheng 2001).

Cheng et al. (1985) investigated the collection efficiency of mesh screens consisting of a single layer of parallel, equidistant woven stainless steel wire with uniform diameter. They found that particle collection efficiency measured experimentally was in good agreement with the filtration theory developed by Kirsch and Fuchs (1967, 1968) and Kirsch and Stechkina (1978) and later adapted for wire screens (Cheng et al. 1980; Cheng and Yeh 1980). The efficiency of a screen of a given thickness is obtained from the calculation of the number of particles of a given dimension deposited on a unit length of fiber (Kirsch and Stechkina 1978). The dimensionless particle deposition rate per unit length of fiber is defined as single-fiber efficiency, and the overall efficiency of a screen is a function of the single-fiber efficiency (Hinds 1999). Compared to regular filter media, stainless steel mesh screens can be cleaned and reused multiple times. However, they are not well suited for chemical analysis, because the metal wires are difficult to digest and analyze separately from the particles that are collected on their surface (Solomon et al. 2001).

Nylon mesh screens offer distinct advantages over stainless steel wire screens. Nylon mesh screens consist of rows of a single layer of parallel, equidistant nylon fibers with uniform diameter interwoven at 90° angles with pore openings ranging between 10 and 180 μm. Nylon mesh screens provide an inexpensive disposable collection substrate that can be ashed or digested for multielemental analysis of the particulate matter collected on the screens, such as atomic absorption spectroscopy and inductively coupled plasma-mass spectrometry (Northington 1987; Grohse 1999). Nylon fibers have been found to leave minimal residual ash and produce no significant spectral interference when ashed for spectrometric examination (Tuchman et al. 2008). Gorbunov et al. (2009) employed nylon screens in a size-selective particle collector. They analyzed the particles collected by the instrument by treating the nylon mesh screens in *aqua regia* and subjecting them to microwave digestion.

The collection efficiency of nylon mesh screens, however, has only been tested for micrometer-sized particles (Yamamoto et al. 2005). The efficiency of nylon mesh screens in collecting submicrometer particles has not been investigated. Furthermore, the ability of theoretical models to estimate collection efficiency of nylon screens for submicrometer particles has not been investigated. Particle size, particle morphology, and several other fluid (flow rate, temperature, and pressure) and screen (thickness, packing density, and fiber diameter) characteristics play an important role and should be factored in the estimation of a screen's collection efficiency when using filtration theory (Friedlander 1958). The effect of morphology on collection efficiency for nylon mesh screens is not known; however, evidence for filters suggests that morphology may have an important effect. Kim et al. (2009) investigated the effects of particle morphology on particle deposition in fibrous filter media and found that agglomerates with mobility diameters larger than 100 nm experience greater collection than spherical particles with the same mobility diameters. For particles smaller than 100 nm, where diffusion is the predominant collection mechanism, collection efficiency was similar regardless of particle morphology (Kim et al. 2009).

The goal of this study was to evaluate filtration theory applied to nylon mesh screens for estimating collection efficiency of particles between 11 and 300 nm. A laboratory study was conducted to experimentally measure pressure drop and single-fiber efficiency by particle size. These data were used to modify filtration theory to improve collection efficiency estimates of nylon mesh screens for particles in this study's size range. A separate laboratory experiment was conducted to determine whether the particle morphology of sub-100 nm affects the collection efficiency of nylon mesh screens and should be included in the filtration theory model.

Methods

Screens

Mesh screens composed of woven nylon 6-6 fibers with pore sizes 60,100, and 180 μm (models NY60, NY1H, NY8H;Millipore Corp., Billerica, MA) and stainless steel screens with twill weave (SS635) were tested in this work (Table 1). Nylon 6-6 is a commonly used synthetic polymer composed of hexamethylene diamine and adipic acid that each contain 6 carbon atoms (hence 6-6). As shown in Figure 1, these mesh screens exhibit uniform openings with fibers arranged at 90° angles. The packing density (a) or solid volume fraction of the nylon screens was calculated as

$$\alpha = \frac{4m_s}{\pi d_s^2 h \rho_s}, \quad [1]$$

where m_s is the mass of the screen measured using a microbalance (Model AX504 Delta Range, Mettler-Toledo Inc., Columbus, OH), d_s is the diameter of the screen reported by the manufacturer, h is the thickness of the screen reported by the manufacturer, and ρ_s is the density of the screen material (i.e., 1.15 g/cm^3 for nylon 6-6).

Experiments

Pressure Drop and Single-Fiber Efficiency—For each pore size, five screens were mounted in each of the 10 stages of the diffusion battery (inner diameter, d_0 = 3.81 cm) of a Diffusional Particle Sizer System (Model 3040, TSI Inc., Shoreview, MN). The pressure drop across all fifty screens was measured with an inclined manometer (Model 400, Dwyer Instruments, Michigan City, IN) as a function of superficial velocity (U_0). Superficial velocity was calculated as $U_0 = Q / A_0$, where Q is the airflow rate through the diffusion battery screen and A_0 is the screen area calculated using d_0. Airflow rate was measured with a mass flowmeter (Model 4199, TSI Inc., Shoreview, MN) and varied from 1 Lpm (U_0 = 1.46 cm/s) to 90 Lpm (U_0 = 131.6 cm/s).

Using the same screen arrangement described above, particle collection efficiency by size was measured at flow rates of 2.5, 4, and 6 Lpm (Figure 2). Flow rates of 4 and 6 Lpm were selected to make this work directly comparable to that of Cheng et al. (1985), whereas the 2.5-Lpm flow rate was selected because it is a commonly used sampling flow rate for industrial hygiene equipment. Stainless steel screens were first tested in the experimental set up for direct comparison with the work of Cheng et al. (1985). Nylon screens were

subsequently mounted in the diffusion battery. Polydisperse ammonium fluorescein aerosol with a count median diameter of 60 nm and geometric standard deviation of 2.0 was generated by nebulizing a solution of 0.19% (by volume) fluorescein ($C_{20}H_{12}O_5$) in 0.01 N ammonium hydroxide with a 6-jet Collison-type nebulizer (BGI, Waltham, MA). This aerosol distribution was selected to cover the wide particle size range between 10 and 300 nm. Compressed air was filtered with a high-efficiency particulate air (HEPA) filter, controlled with a regulator, and fed into the nebulizer. The polydisperse aerosol was passed through a diffusion dryer (Model 3062, TSI Inc., Shoreview, MN) and a charge neutralizer (Model 3054, TSI Inc., Shoreview, MN). A scanning mobility particle sizer (SMPS—Model 5.4, Grimm Technology, Douglasville, GA) was used to measure number concentrations by size entering Stage 0 of the diffusion battery (no screens, C_{in}) and exiting even stages between Stage 2 and Stage 10 (C_{out}) in the sequence: 0-2-0-4-0-6-0-8-0-10. After one sequence, new screens were placed in the diffusion battery and the measurements were repeated to obtain a total of three replicates for each pore size and flow rate. The switching valve of the Diffusional Particle Sizer System was used to sequentially connect each exit port of the even stages of the diffusion battery to the SMPS.

Aerosol penetration (P) was calculated for SMPS midpoint diameters between 10 and 100 nm at 10-nm intervals, and 150, 200, and 300 nm as $P_{i,j,k} = C_{out,\ i,j,k}/C_{in,\ i,j,k}$, where i is the diffusion battery stage number (2 through 10), j is the SMPS midpoint diameter, and k is the replicate (1 through 3). Following Cheng et al. (1985), the logarithm with base 10 of aerosol penetration by size was plotted relative to the total number of screens the aerosol passed in a corresponding stage i. Linear regression of the form $\log(P_{j,k}) = m_{j,k}\,n$, where n is the number of screens, was performed on the plotted data and single-fiber efficiency (η) by size was calculated from the slope (m) as

$$\eta_{j,k} = -m_{j,k}\ln 10/B, \quad [2]$$

where $B = 4ah/(\pi(1-a)d_f)$ and d_f is the fiber diameter. Mean single-fiber efficiencies of the three replicates were then plotted as a function of particle diameter, compared to estimates from theory (Cheng et al. 1985), and assessed for fit.

Effect of Morphology on Collection Efficiency—The effect of morphology on the collection efficiency of nylon mesh screens was observed for highly fractal-like and spherical particles using the experimental setup shown in Figure 3. Following Ku and Maynard (2006), silver (Ag) particles of varying morphology were generated using two horizontal tube furnaces in series. The first furnace (Lindberg/Blue, Laboratory Tube Furnace STF55433C) was operated at 1200°C with pure nitrogen (purity level 99.999%) at an airflow of 1.0 Lpm passed over silver wire (purity level 99.9%) placed in a ceramic boat. A digital mass flow controller (Model 0154, Brooks Instrument, Hatfield, PA) was used to maintain a constant nitrogen flow rate. The aerosol leaving the first furnace was passed through a coagulation chamber (residence time ~40 s) where the aerosol cooled to form chain agglomerates with an open structure (Figure 4a). For highly fractal tests, the second furnace (Blue TF55035A, Blue M, New Columbia, PA) was operated at room temperature (furnace off). Alternatively, for spherical particle tests, the second furnace was operated at

600°C to sinter the agglomerates so that they would form spheres when cooled (Figure 4b). The particles shown in Figure 4a and b were collected with an electrostatic precipitator located in place of the filter holder in the setup shown in Figure 3 and were analyzed under transmission electron microscopy. Filtered compressed air at 1.5 Lpm was added after the second furnace to bring the flow rate to the commonly used sampling flow rate for industrial hygiene equipment of 2.5 Lpm.

Collection efficiency was measured for screens with 60-μm pore size (NY60), at 2.5 Lpm, for 15, 40, and 100 nm mobility diameters, and for spherical and highly fractal-like particle morphologies. An electrostatic classifier (Model 3080L, TSI Inc., Shoreview, MN) was used to select the mobility diameters. A polonium-210 radioactive source (Model 2U500, NRD LLC, Grand Island, NY) was used to neutralize the aerosol before it was passed through a stack of either five NY60 screens (for the 20 nm tests) or twenty NY60 screens (for the 40 and 100 nm tests). New screens were passed under a polinium-210 source (Model 2U500, NDR LLC, Grand Island, NY) for 10 s and loaded in the filter holder before each test. A condensation particle counter (Model 3022A, TSI Inc, Shoreview, MN) was used to measure monodisperse aerosol concentration for 120 s before (C_{in}) and after (C_{out}) passing through the screens. This measurement procedure was repeated three times. Collection efficiency was calculated as $E = 1 - $ (average C_{out}/average C_{in}), where the average represents the mean of the concentration over 120 s.

Modification of Theory—Single-fiber efficiency of screens can be expressed as the sum of the individual efficiencies for diffusion, interception, and a correction term for diffusion and interception (Kirsch and Stechkina 1978; Cheng et al. 1980, 1985). Theoretical single-fiber efficiency of the nylon mesh screens was estimated following Cheng et al. (1985) as:

$$\eta = 2.7 Pe^{-2/3} + 2(2\kappa)^{-1} R_2 + 1.24 \kappa^{-1/2} Pe^{-1/2} R^{2/3}, \quad [3]$$

where Pe is the Peclet number ($Pe = d_f U_0/D$), $\kappa = -(1/2)\ln c - 0.75 + c - (c^2/4)$, $c = 2\alpha/\pi$, R is the interception parameter ($R = d_p/d_f$), U_0 is the superficial velocity, and d_p is the particle diameter. D is the diffusion coefficient $D = k_B T Cc/6 \pi \mu d_p$, where k_B is the Boltzmann constant, T is the temperature, Cc is the slip correction factor, and μ is the air viscosity. The coefficients of each term in Equation (3) were originally determined through laboratory experiments performed by Kirsch and Fuchs (1968).

The experimental single-fiber efficiency values for a given particle size, calculated using Equation (2), were used to modify the coefficients of each term in Equation (3) (2.7, 2, and 1.24). New coefficients were determined to minimize the sum of the square error (SSE) between theoretical and experimental single-fiber efficiency values. The solver function (MS Excel, Microsoft Corp., Redmond, WA) was used to minimize the SSE by iteratively changing the three coefficients in Equation (3).

Results and Discussion

Pressure Drop and Collection Efficiency

A linear relationship was observed between pressure drop and superficial velocity for all pore sizes over the velocity range from 1 to 130 cm/s (Figure 5). A linear relationship between pressure drop and superficial velocity is an underlying assumption of a filtration theory for calculation of particle collection efficiency that is based on single-fiber efficiency (Cheng et al. 1985).

Mean experimental single-fiber efficiencies as a function of particle diameter with 95% confidence interval error bars are provided in Figure 6 (closed symbols) for NY60 screens at 6 Lpm. The theoretical expression of Equation (3) (solid line) is in good agreement with estimates of single-fiber efficiency for nylon net screens for particles between 40 and 150 nm, where theory was within the 95% confidence intervals of the experimental data points. Theoretical estimations, however, were outside of the 95% confidence intervals of the experimental data for particles smaller than 40 nm, where efficiency was over-estimated, and larger than 150 nm, where efficiency was underestimated. The explanation for these findings is unknown for particles smaller than 40 nm. For particles larger than 150 nm, the effect of the impaction mechanism, assumed to be negligible by Equation (3), was tested following the single-fiber efficiency expression proposed by Cheng et al. (1980). This single-fiber efficiency expression includes an inertial impaction term in addition to the diffusion and direct interception terms. The inclusion of the inertial impaction term yielded the same single-fiber efficiency estimations as those obtained with Equation (3) for particles larger than 150 nm for all mesh sizes tested. Inertial impaction was therefore ruled out as a possible explanation of the discrepancy between theoretical and experimental single-fiber efficiency values for particles larger than 150 nm.

The theoretical estimations of the single-fiber efficiency model tested by Cheng et al. (1985) on stainless steel screens have been used to determine the number and pore size of nylon mesh screens for a size-selective collector for particles smaller than 0.25 μm (Gorbunov et al. 2009). The collection efficiency of nylon mesh screens, however, has only been investigated for micrometer-sized particles ranging between 0.3 and 100 μm (Yamamoto et al. 2005). In their work, Yamamoto et al. (2005) found high variability in experimental data and discrepancies between theoretical and experimental collection efficiencies. Particularly, they found that the theoretical estimations were higher than the experimental collection efficiencies for particles smaller than 5 μm and larger than 20 μm. The present tests and evaluations of collection efficiency for sub-300 nm particles, coupled with the analytical advantages of the nylon fibers, provide valuable information for future uses of nylon mesh screens as particle collection media.

Effect of Morphology on Collection Efficiency

The results of the silver particle morphology tests are summarized in Table 2. For each mobility size, morphology affected efficiency by less than 4%. No specific morphology was found to affect overall efficiency more than another. For the 15-nm aerosol, highly fractal-like particles had smaller collection efficiency (34.3%) than spherical particles (37.9%).

Conversely, for 40 and 100-nm mobility sizes, the spherical particles had smaller collection efficiency (43.9% and 23.4%, respectively) while highly fractal-like particles had larger collection efficiency (45.6% and 24.0%, respectively).

Highly fractal-like particles have larger interception lengths than spherical particles; however, when compared to the screen fiber diameter (33 μm), the particles studied in these tests were so small (100 nm) that interception may not play a significant role in their collection. Visual comparison between fiber diameter and particle size can be observed in the inset in Figure 1, showing fluorescein nanoparticles deposited on an NY60-screen fiber. These efficiency similarities are consistent with the findings for fibrous filters of Kim et al. (2009), who found that for particles smaller than 100 nm, penetration through filters was similar regardless of particle morphology.

These results have implications for the evaluation of theory. A significant effect of morphology on the screen's overall efficiency would have warranted the inclusion of this factor in the theoretical model. These tests confirmed the negligible effect of morphology on collection efficiency of sub-100 nm particles and validated its exclusion from theoretical estimation models.

Modification of Theory

The experimental collection efficiency data were used to empirically modify the coefficients of Equation (3). These coefficients were estimated by minimizing the SSE between theoretical and experimental data. The SSE values for the theoretical model with the original coefficient (Equation (3)) and modified theory with new coefficients are reported in Table 3. The modified coefficients are 2.3, 2, and 4.3, and hence the modified single-fiber efficiency theory is expressed as

$$\eta = 2.3Pe^{-2/3} + 2(2\kappa)^{-1}R^2 + 4.3\kappa^{-1/2}Pe^{-1/2}R^{2/3}. \quad [4]$$

For all screen types and flow rates tested, the SSE was lower for the theory with the modified coefficients than for that with the original coefficients (Table 3), indicating improved fit. The SSE was at least one order of magnitude lower when calculated using Equation (4) for all screens and flow rates with the exception of the NY60 screens at 2.5 Lpm flow rate, where the decrease was threefold.

The improved agreement between the modified single-fiber efficiency and the experimental data is visible in Figure 6, where the dotted line represents the modified theoretical estimations of Equation (4). Figure 7 presents mean experimental single-fiber efficiency and theoretical estimations calculated using Equation (4) for all pore sizes and flow rates tested, showing that the theoretical values estimated with the modified coefficients fall within the 95% confidence interval error bars of the experimental values. The new model (Equation (4)) can therefore be used for estimating theoretical efficiency of nylon net screens if the physical dimensions of the screens (i.e., screen thickness, fiber diameter, and packing density) are known as $E = 1 - \exp(-\eta Bn)$, where η is Equation (4) and n is the number of screens.

Estimates of single-fiber efficiency made with the original theory (Equation (3)) fell within the 95% confidence interval of experimental data only for particles between 40 and 150 nm for both nylon and stainless steel screens. The tests performed with the stainless steel screens allowed direct comparison of our results with those of Cheng et al. (1985), who found that this model fit experimental values well for stainless steel screens for all particle sizes tested from 0.22 to 0.95 μm. Deviation of experiment from theory was expected for nylon but not for stainless steel screens.

The deviation observed for stainless steel screens may be due to differences between the experimental setup and the instrumentation used in this study and that of Cheng et al. (1985). Cheng and coworkers generated polydisperse oleic acid aerosol that was subsequently classified to yield monodisperse fractions. Aerosol concentrations were measured simultaneously with a condensation nucleus counter and a Faraday cup with an electrometer, and the slopes obtained from the linear regression on aerosol penetration by number of screens of the two sets of data were averaged prior to the calculation of single-fiber efficiency. This method yielded one single-fiber efficiency value per particle size and no indication of the variability within measurements for each particle size. In our experiments, we generated polydisperse ammonium fluorescein aerosol and measured aerosol concentration by size using an SMPS. This method greatly reduced the number of experiments and allowed us to obtain triplicate measurements for each particle size. Linear regression was performed on each set of data and the linear regression slopes were not averaged prior to the calculation of single-fiber efficiency. The single-fiber efficiency values obtained from the slopes were averaged and the repeated measurements were used to estimate 95% confidence intervals around the mean efficiencies.

A similar approach to developing empirical efficiency models has been taken by Wang et al. (2007). In a study that investigated the filtration efficiency due to diffusion of standard filters for particles ranging between 3 and 400 nm, they compared experimental data with a theoretical filtration model similar to the one used in this study. Wang et al. (2007) averaged the model coefficients obtained from experimental data of four filter medias to develop a new model that better estimates the filter's collection efficiency. Unlike nylon net screens, standard filters have nonhomogeneous fiber diameters that make it difficult to theoretically express filtration efficiency.

There are some limitations to this work. The modified single-fiber efficiency model provided in this study (Equation (4)) may not apply to particle sizes outside of the range observed in this study (10–300 nm). Additionally, nylon fibers may develop and retain static electricity charges that may affect the collection efficiency of the screens. The effect of these charges on particle collection efficiency was not investigated in this study. The effects of particle morphology were tested on silver particles; therefore, the results obtained may not apply to fibrous particles such as carbon nanotubes.

Conclusions

The pressure drop and particle collection efficiency were measured experimentally for 3 pore sizes of nylon mesh screens. The effects of particle morphology on collection

efficiency of the screens were also evaluated. No substantial effects on efficiency changes were found for spherical and highly fractal-like silver particles. Single-fiber efficiency of the nylon mesh screens was calculated from the experimental data and compared to the theoretical estimations for fibrous filters of Kirsch and Stechkina (1978) adapted for mesh screens by Cheng et al. (1980). The results of this comparison indicated that the theoretical estimations were in good agreement with the experimental data for particles between 40 and 150 nm, but the experimental data deviated from theory for particles smaller than 40 nm and larger than 150 nm. A modified theory to estimate collection efficiency of nylon mesh screens was generated by empirically modifying the model's coefficients. The modified theory was found to better match the experimental data and fell within the 95% confidence interval limits of the experimental data.

Nylon mesh screens provide a low-cost, disposable collection surface suitable for collection of nanoparticles and are compatible with a wide range of analysis methods. The ability to accurately estimate collection efficiency of particles and of analyzing their composition with minimal interference from the nylon fibers makes nylon mesh screens an ideal collection substrate for nanoparticles. The use of nylon mesh screens as diffusion material may help better understand and estimate workers' exposure to nanoparticles.

Acknowledgments

References

Cheng, YS. Condensation Detection and Diffusion Size Separation Techniques. In: Baron, PA.; Willeke, K., editors. Aerosol Measurements: Principles, Techniques, and Applications. 2nd. John Wiley & Sons; New York: 2001. p. 569-601.

Cheng YS, Keating JA, Kanapilly GM. Theory and Calibration of a Screen-Type Diffusion Battery. J Aerosol Sci. 1980; 11:549–556.

Cheng YS, Yeh HC. Theory of a Screen-Type Diffusion Battery. J Aerosol Sci. 1980; 11:313–320.

Cheng YS, Yeh HC, Brinsko KJ. Use of Wire Screens as a Fan Model Filter. Aerosol Sci Technol. 1985; 4:65–174.

Emi H, Wang CS, Tien C. Transient Behavior of Aerosol Filtration in Model Filters. AIChE J. 1982; 28:397–405.

Friedlander SK. Theory of Aerosol Filtration. Ind Eng Chem. 1958; 50(8):1161–1164.

Fu TH, Cheng MT, Shaw DT. Filtration of Chain Aggregate Aerosols by Model Screen Filter. Aerosol Sci Technol. 1990; 13:151–161.

Gentry JW, Choudhary KR. Collection Efficiency and Pressure Drop in Grid Filters of High Packing Densities at Intermediate Reynolds Numbers. J Aerosol Sci. 1975; 6:277–290.

Gorbunov B, Priest ND, Muir RB, Jackson PR, Gnewuch H. A Novel Size-Selective Airborne Particle Size Fractionating Instrument for Health Risk Evaluation. Ann Occup Hyg. 2009; 53(3):225–237. [PubMed: 19279163]

Grohse, PM. Trace Element Analysis of Airborne Particles by Atomic Absorption Spectroscopy, Inductively Coupled Plasma-Atomic Emission Spectroscopy, and Inductively Coupled Plasma-Mass Spectrometry. In: Landsberger, S.; Creatchman, M., editors. Environmental Analysis of Airborne Particles Advances in Environmental, Industrial and Process Control Technologies. Vol. 1. Gordon and Breach Science Publishers; Amsterdam, The Netherlands: 1999. p. 1-65.

Hinds, WC. Aerosol Technology: Properties, Behavior, and Measurements of Airborne Particles. John Wiley & Sons; New York: 1999.

Kim SC, Wang J, Emery MS, Shin WG, Mulholland GW, Pui DYH. Structural Property Effect of Nanoparticle Agglomerates on Particle Penetration Through Fibrous Filter. Aerosol Sci Technol. 2009; 43:344–355.

Kirsch AA, Fuchs NA. Studies of Fibrous Aerosol Filters—II. Pressure Drops in Systems of Parallel Cylinders. Ann Occup Hyg. 1967; 10:23–30. [PubMed: 6043103]

Kirsch AA, Fuchs NA. Studies of Fibrous Filters—III: Diffusional Deposition of Aerosol in Fibrous Filters. Ann Occup Hyg. 1968; 11:299–304. [PubMed: 5721714]

Kirsch, AA.; Stechkina, IB. The Theory of Aerosol Filtration with Fibrous Filters. In: Shaw, DT., editor. Fundamentals of Aerosol Science. John Wiley & Sons; New York: 1978. p. 165-256.

Ku BK, Maynard AD. Generation and Investigation of Airborne Silver Nanoparticles with Specific Size and Morphology by Homogeneous Nucleation, Coagulation and Sintering. J Aerosol Sci. 2006; 37:452–470.

Northington DJ. Inductively Coupled Plasma-Mass Spectrometry for the Analysis of Metals in Membrane Filters. Am Ind Hyg Assoc J. 1987; 48(12):977–979.

Sinclair D, Hoopes GS. A Novel Form of Diffusion Battery. Am Ind Hyg Assoc J. 1975; 36:39–42. [PubMed: 1111266]

Solomon, PA.; Norris, G.; Landis, M.; Tolocka, M. Chemical Analysis Methods for Atmospheric Aerosol Components. In: Baron, PA.; Willeke, K., editors. Aerosol Measurement: Principles, Techniques, and Applications. John Wiley & Sons; New York: 2001. p. 261-293.

Tuchman DP, Volkwein JC, Vinson RP. Implementing Infrared Determination of Quartz Particulates on Novel Filters for a Prototype Dust Monitor. J Environ Monit. 2008; 10:671–678. [PubMed: 18449405]

Wang J, Chen DR, Pui DYH. Modeling of Filtration Efficiency of Nanoparticles in Standard Filter Media. J Nanoparticle Res. 2007; 9:109–115.

Yamamoto N, Kumagai K, Fujii M, Shendell DG, Endo O, Yanagisawa Y. Size-Dependent Collection of Micrometer-Sized Particles Using Nylon Mesh. Atmos Environ. 2005; 39:3675–3685.

Yeh HC, Cheng YS, Orman MM. Evaluation of Various Types of Wire Screens as Diffusion Battery Cells. J Colloid Interface Sci. 1982; 86:12–16.

Author Manuscript

Author Manuscript

Author Manuscript

Author Manuscript
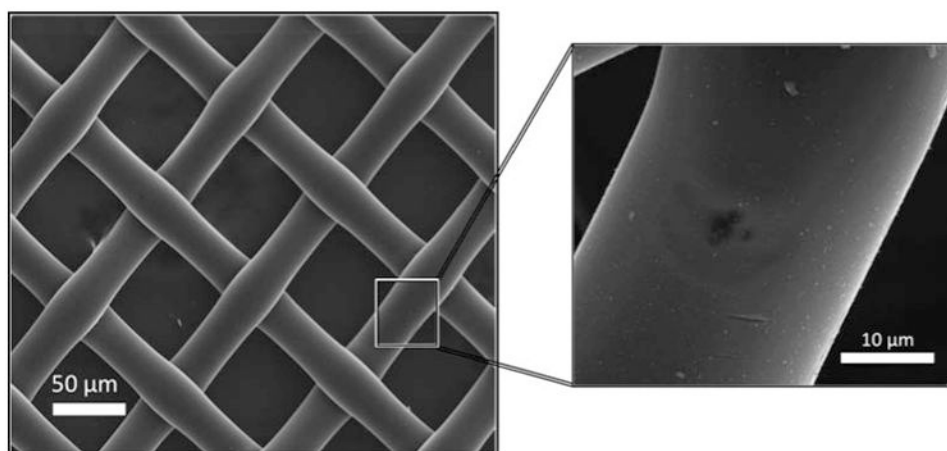
Fig. 1.
Scanning electron microscopy image of NY60 nylon mesh screen with insert showing fluorescein loading (white spots) on a single fiber.
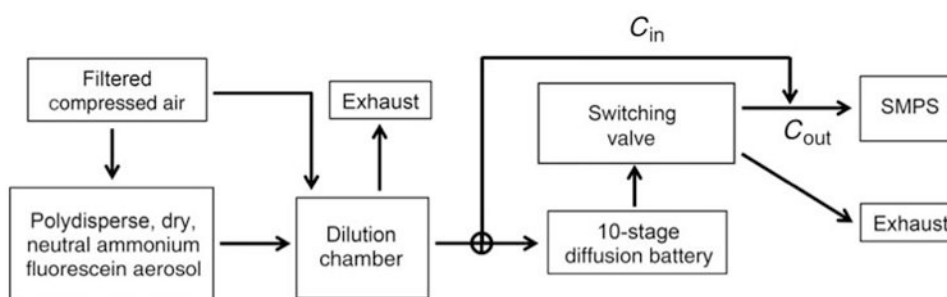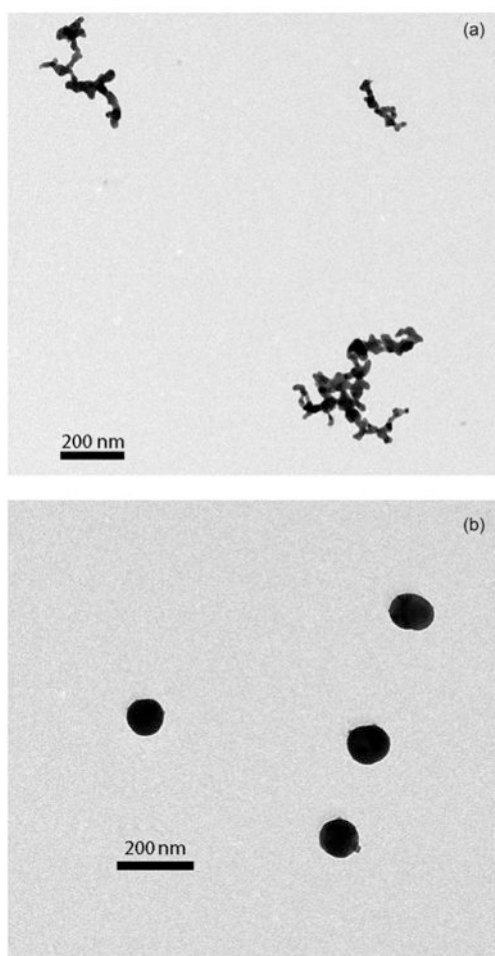
Fig. 2.
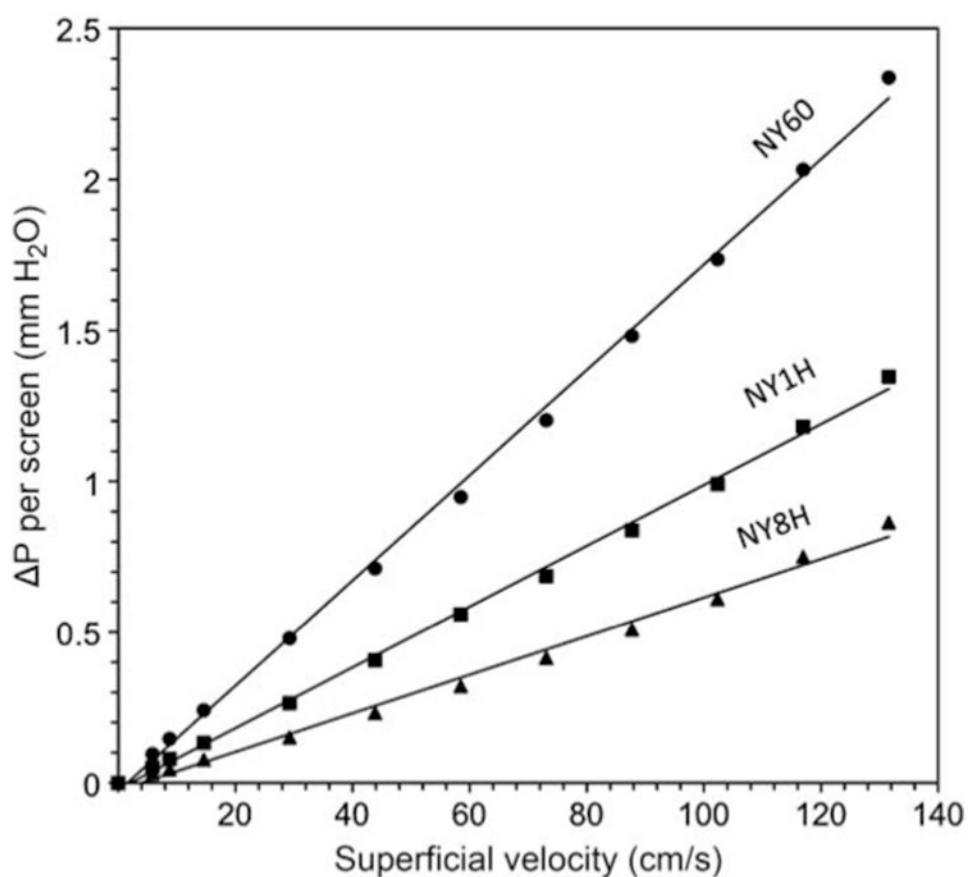Experimental setup for particles collection efficiency tests.
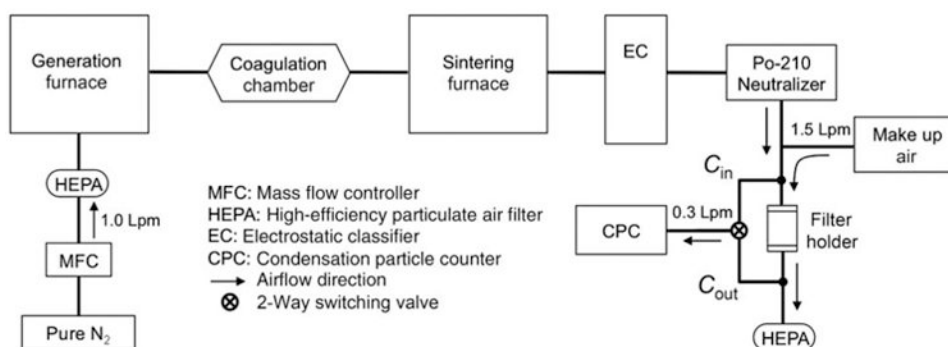
Fig. 3.
Experimental setup for evaluation of particle morphology on collection efficiency (adapted from Ku and Maynard 2006).
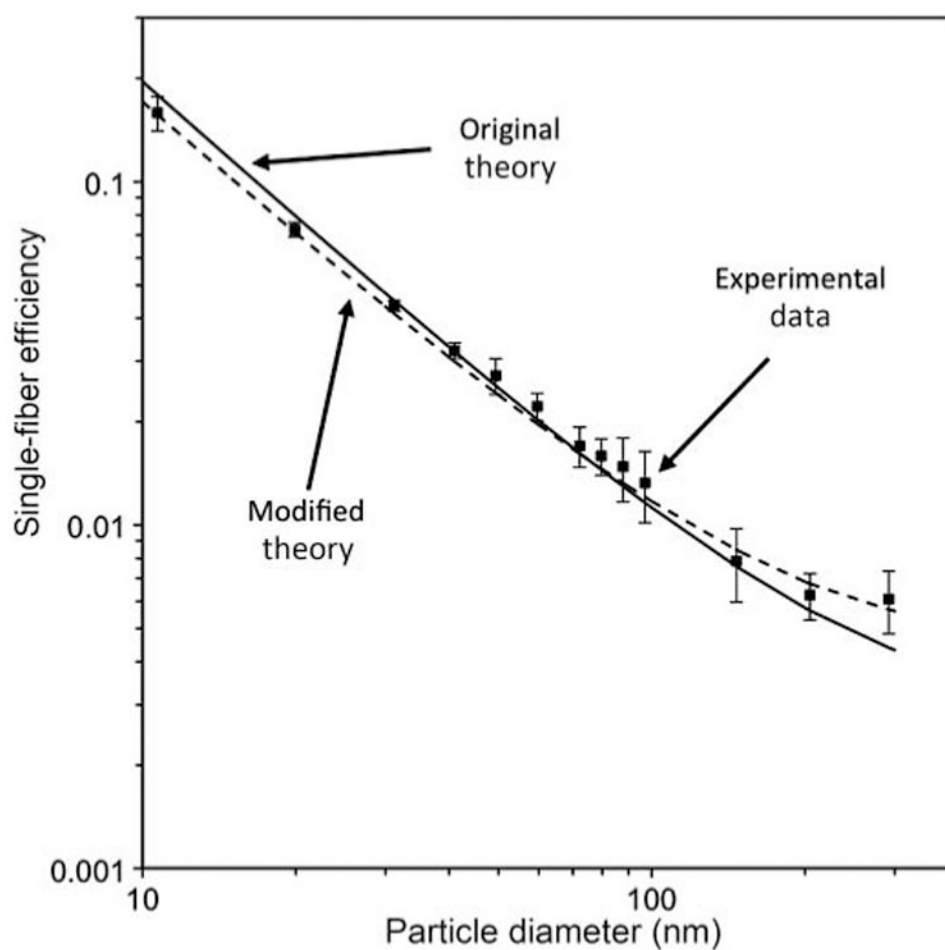
Fig. 4.
Transmission electron microscopy images of (a) highly fractal Ag nanoparticles (no sintering) and (b) spherical Ag nanoparticles (600°C sintering).
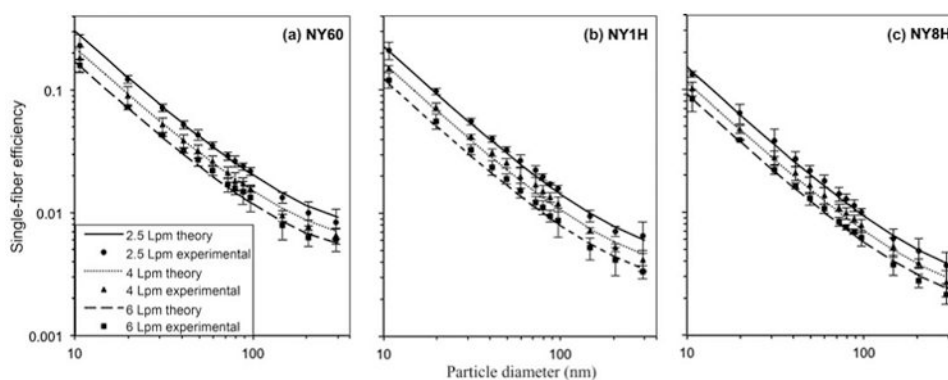
Fig. 5.
Pressure drop per screen as a function of superficial velocity. Solid line is a linear regression through data points.

Fig. 6.
Experimental data with comparison of original and modified single-fiber efficiency theory for NY60 screens at 6 Lpm. Error bars represent 95% confidence intervals.

Fig. 7.
Theoretical (Equation (4)) and experimental single-fiber efficiency of (a) NY60 screens, (b) NY1H screens, and (c) NY8H screens. Error bars represent 95% confidence intervals.

Table 1

Physical specifications of the nylon mesh screens

Screen model	Pore size (μm)	Open area (%)	Thickness, h (μm)	Fiber diameter, d_f (μm)	Mass (SD) (mg)	Packing density, a
NY60	60	41	50	33	31.9(0.5)[*]	0.32
NY1H	100	44	80	51	45.5 (0.2)[*]	0.29
NY8H	180	47	135	83	83.4 (0.3)[**]	0.31
SS635	~ 60	n/a	50[***]	20[***]	n/a	0.35[***]

[*] From Yamamoto et al. (2005).

[**] Weighed by microbalance ($n = 8$).

[***] From Cheng et al. (1985).

n/a—not available.

Table 2

Effects of particle morphology on collection efficiency of NY60 screens

Particle diameter (nm)	Number of screens	Collection efficiency (*SD*) (%)	
		Spherical	**Highly fractal-like**
15	5	37.9 (0.6)	34.3 (0.7)
40	20	43.9(0.1)	45.6 (0.5)
100	20	23.4 (0.3)	24.0 (0.2)

Table 3

Sum of squares error between experimental single-fiber efficiency values and theoretical models (original and modified)

Screen type	Flow rate (Lpm)	Sum of squares error	
		Original theory (Equation (3))	Modified theory (Equation (4))
NY60	2.5	8.65×10^{-3}	2.43×10^{-3}
	4	3.08×10^{-3}	5.59×10^{-4}
	6	4.86×10^{-4}	3.83×10^{-5}
NY1H	2.5	9.50×10^{-4}	5.07×10^{-5}
	4	6.53×10^{-4}	5.57×10^{-5}
	6	1.77×10^{-4}	5.25×10^{-5}
NY8H	2.5	8.43×10^{-4}	5.87×10^{-5}
	4	4.41×10^{-4}	2.39×10^{-5}
	6	2.11×10^{-4}	4.46×10^{-6}
SS635	2.5	1.32×10^{-2}	3.76×10^{-3}
	4	2.95×10^{-3}	2.23×10^{-4}
	6	3.54×10^{-3}	8.58×10^{-4}